Nickel is a Different Pickle: Trends in Water Oxidation Catalysis for Molecular Nickel Complexes

Joeri Hessels,[a] Eduard Masferrer-Rius,[b] Fengshou Yu,[a] Remko J. Detz,[c] Robertus J. M. Klein Gebbink,[b] and Joost N. H. Reek*[a]

The development of novel water oxidation catalysts is important in the context of renewable fuels production. Ligand design is one of the key tools to improve the activity and stability of molecular catalysts. The establishment of ligand design rules can facilitate the development of improved molecular catalysts. In this paper it is shown that chemical oxidants can be used to probe oxygen evolution activity for nickel-based systems, and trends are reported that can improve future ligand design. Interestingly, different ligand effects were observed in comparison to other first-row transition metal complexes. For example, nickel complexes with secondary amine donors were more active than with tertiary amine donors, which is the opposite for iron complexes. The incorporation of imine donor groups in a cyclam ligand resulted in the fastest and most durable nickel catalyst of our series, achieving oxygen evolution turnover numbers up to 380 and turnover frequencies up to 68 min^{-1} in a pH 5.0 acetate buffer using Oxone as oxidant. Initial kinetic experiments with this catalyst revealed a first order in chemical oxidant and a half order in catalyst. This implies a rate-determining oxidation step from a dimeric species that needs to break up to generate the active catalyst. These findings lay the foundation for the rational design of molecular nickel catalysts for water oxidation and highlight that catalyst design rules are not generally applicable for different metals.

Introduction

The development of novel catalysts helps to further improve the electrochemical production of renewable fuels, such as H_2 and MeOH.[1,2] These energy carriers are suggested to play a role in the transition to an economy based on renewable resources, both as a storage option in the electricity sector and as a fuel in, for example, the transport sector, or as feedstock for the chemical industry.[3–6] Hydrogen can be produced via proton reduction, while methanol or other carbon-based fuels could be produced by CO_2 reduction.[7–13] For both these processes, water oxidation is required to supply electrons and protons. This oxidation reaction is generally the limiting factor for efficient and stable devices.[14–19] Important parameters of water oxidation catalysts (WOCs) are the overpotential at which they operate, their activity, and their stability. In industrial settings, heterogeneous catalysts are used for the water oxidation reaction.[20–22] In proton-exchange membrane (PEM) cells, iridium is often used as catalyst at the anode, while in alkaline electrolyzers the catalyst is typically based on nickel.[3,23,24] Inspired by photosystem II in nature,[25–28] a significant amount of research has been devoted to develop molecular WOCs. These systems have the advantage of being easier to study, as well as being more active per metal center.[29] Interestingly, by varying the ligand framework of a molecular catalyst, performance can be enhanced by several orders of magnitude.[30–32] In addition to high water oxidation activity, a catalyst also has to withstand the highly oxidative potentials that are required to oxidize water. The postulation of design rules can aid the development of effective catalysts that meet the requirements for this challenging reaction. Llobet and co-workers recently published an excellent review on ligand design for robust WOCs with high activity.[33] To arrive at a successful WOC, the ligand should coordinate strongly to the catalytically active metal to prevent substitution and be oxidatively stable to prevent ligand oxidation. In addition, the complex needs to be able to access high oxidation states at moderate potentials, while allowing for a favorable water oxidation mechanism. As the oxygen evolution reaction requires two water molecules and the transfer of four electrons and four protons, it proceeds via a relatively complicated mechanism.[16,34,35] The mechanism also influences the overpotential required for water oxidation catalysis. The minimal overpotential of a catalyst that operates via the mononuclear water nucleophilic attack mechanism is dictated by scaling relations resulting in a minimum overpotential of around 300 mV.[34] The dinuclear radical coupling reaction does not suffer from this minimal overpotential but is

[a] Dr. J. Hessels, Dr. F. Yu, Prof. Dr. J. N. H. Reek
Homogeneous, Supramolecular and Bio-Inspired Catalysis, Van 't Hoff Institute for Molecular Sciences
University of Amsterdam
Science Park 904, 1098 XH Amsterdam (The Netherlands)
E-mail: j.n.h.reek@uva.nl

[b] E. Masferrer-Rius, Prof. Dr. R. J. M. Klein Gebbink
Organic Chemistry & Catalysis, Debye Institute for Nanomaterials Science
Utrecht University
Universiteitsweg 99, 3584 CG Utrecht (The Netherlands)

[c] Dr. R. J. Detz
Current address: TNO Energy Transition, Energy Transition Studies, Radarweg 60, 1043 NT Amsterdam (The Netherlands)

ChemSusChem

Full Papers
doi.org/10.1002/cssc.202002164

**Chemistry
Europe**
European Chemical
Societies Publishing

more sensitive to concentration differences. The use of supramolecular strategies in WOC design seems promising. For example, increasing the local concentration of catalysts by confinement improved the activity of a ruthenium catalyst by two orders of magnitude.[36] In addition, π-π stacking can also pre-organize catalysts that operate via a dinuclear mechanism.[37] Ruthenium-based WOCs are some of the most potent[39] and progress in this field has recently been reviewed by Kamdar and Grotjahn.[38] Chemical oxidants, like cerium(IV) ammonium nitrate (CAN), are often used for comparing catalysts, as they allow for adequate comparison between catalytic systems at identical conditions.[40] For iridium-based catalysts, ligand design trends are observed by the use of chemical oxidants in water oxidation, as for example shown by Crabtree and co-workers as well as Bernhard and co-workers.[41,42]
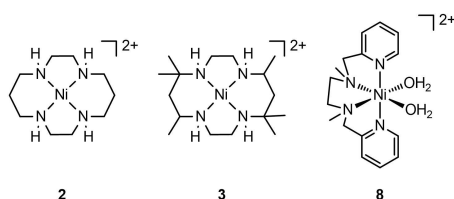
Ruthenium- and iridium-based systems still represent the most effective molecular WOCs,[39–43] and current catalysts based on first-row transition metals are often less active and less stable.[14,44] In addition, WOCs based on first-row transition metals usually also require a higher potential to drive the oxygen evolution reaction. As these metals are orders of magnitude cheaper, sufficiently available for large scale applications, and also because nature's catalysts are based on first-row metals, a significant amount of work has been devoted to the development of molecular WOCs based on manganese, iron, cobalt, and copper.[14,45–48] As an example, Lloret-Fillol et al. used chemical oxidants to evaluate iron complexes for water oxidation and reported one of the most robust iron-based catalyst to date. Structure-activity relationships suggest that active iron-based catalysts require two *cis*-vacant sites.[49] Interestingly, molecular nickel complexes have been less explored for water oxidation,[14] while commercial alkaline electrolyzers contain heterogeneous nickel-based catalysts.[24,50] In 2014, the first electrochemically active nickel-based molecular WOC was published, which employs the cyclam-like meso-ligand (**3**, Figure 1).[51] In two follow-up papers, a pyridine-based ligand system was also shown to work under acidic and neutral pH conditions (**8**, Figure 1).[52,53] Recently, the same authors also published structure-activity relations between several meso-like ligands. The trend indicates that additional methylation of the backbone has a favorable effect.[54] Meyerstein and co-workers showed that cyclam complex **2** is also active in water oxidation (Figure 1).[55] Several other groups also demonstrated the use of molecular nickel complexes for water oxidation using porphyrin-, cyclam-, oxamide-, and pyridine-based ligand

frameworks.[56–63] In all of these contributions water oxidation catalysis was reported using electrochemistry, which gives information on the potential at which water oxidation catalysis starts and reaction rates under specific conditions. However, as these publications all use various pH and buffer conditions, a proper comparison of the different catalysts is difficult. Furthermore, a study on systematic variations of the ligand framework to provide insight in structure-activity relationships for nickel-based water oxidation catalysts is missing. In this work we investigate a series of novel and previously reported nickel complexes as water oxidation catalysts under identical conditions. Inspired by the progress in ruthenium-, iridium-, and iron-based WOCs (see above),[40–42,49,64] we used chemical oxidants for the evaluation of the activity of these nickel-based complexes. From the results we extract design rules, which appear to be different when compared to those found for other metals. We hope that these design rules will advance the field of nickel-based water oxidation catalysis.
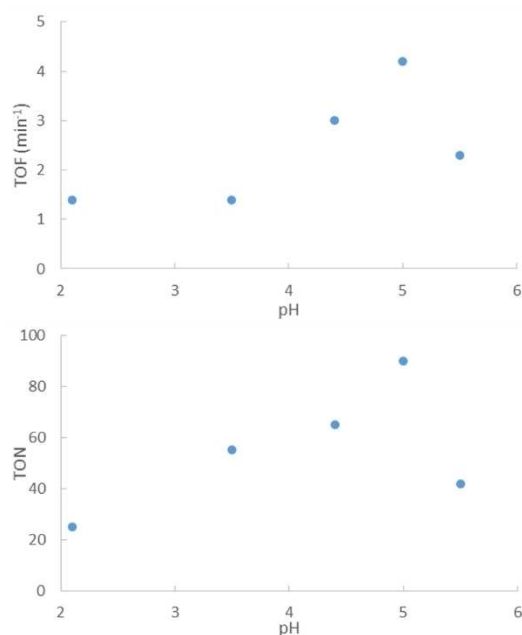
Results and Discussion

In 2014 Lau and co-workers reported the use of $[Ru(bpy)_3]^{3+}$ as chemical oxidant for the evaluation of several nickel-based catalysts at a pH of 8.[65] They showed that ligands had an adverse effect on the catalytic activity, and the nickel salt Ni$(NO_3)_2$ appeared most active. This activity is likely caused by nickel nanoparticles, which are rapidly formed under these conditions. The formation of nanoparticles at basic pH values is more commonly observed for first-row transition metal complexes used for water oxidation catalysis.[61,62,66] We are interested in the use of chemical oxidants on a pH scale ranging from 1 to 7 to drive nickel-based water oxidation catalysis. These conditions are more compatible with proton reduction catalysis in a full water splitting cell. We applied the Oxodish method, previously developed by our group,[67] to rapidly evaluate the water oxidation activity of various nickel complexes with chemical oxidants. Both in an unbuffered and in phosphate-buffered (pH 7.0) solution, our nickel complexes do not reveal any activity with oxidants such as CAN and sodium periodate, which are typically used to examine ruthenium-, iridium-, and iron-based systems (Supporting Information, Table S1).[40,42,49,68,69] Interestingly, in a pH 4.5 acetate buffer with the two-electron sacrificial oxidant Oxone, which is known to drive water oxidation in manganese-, iron-, and ruthenium-based systems,[64,71–77] nickel cyclam **2** and nickel BPMEN complex **8** evolve oxygen (Figure 1 and Supporting Information, Figure S1). In a control experiment we showed that nickel salts and NiO$_x$ nanoparticles remain inactive under these conditions (Supporting Information, Table S1).

As water oxidation is generally pH sensitive, we performed catalysis experiments at various degrees of acidity using nickel cyclam **2** as a model catalyst (Figure 2). To determine the maximum turnover numbers (TONs) and turnover frequencies (TOFs) of our nickel-based WOCs, we used a manometer to quantify the pressure change as a measure of evolved oxygen gas.[42,78,79] Catalyst **2** evolves oxygen at a rate of approximately

Figure 1. Examples of nickel complexes studied in literature for water oxidation.

ChemSusChem

Full Papers
doi.org/10.1002/cssc.202002164

Chemistry Europe
European Chemical
Societies Publishing

Figure 2. TOFs per minute (top) and TONs (bottom) of oxygen evolution by 0.10 mM nickel cyclam **2** at various pH values in a 0.50 M acetate buffer using 0.10 M Oxone as oxidant.

Figure 3. Oxygen evolution by 0.10 mM of nickel complexes **1** (blue), **2** (purple), **3** (green), **6** (grey), and Ni(ClO$_4$)$_2$ (black) at a pH of 5.0 in a 0.50 M acetate buffer using 0.10 M Oxone as oxidant (top, TON determined by manometry). Structure of complexes **1** and **6** (bottom); the structures of **2** and **3** are depicted in Figure 1.

1.4 turnovers min^{-1}, both at pH 2.1 and 3.5. At pH 4.4, the rate increases to 3 turnovers min^{-1}. The catalyst displays the highest rate at pH 5, with 4.2 turnovers per minute. At even lower acidity, above pH 5.0, the catalyst is slower, reaching a TOF of 2.3 min^{-1} at pH 5.5. The trend in maximum TON is similar to the trend in TOF (Figure 2). As cyclam-based nickel complex **2** has the highest rate for oxygen evolution at pH 5, we performed the remainder of our experiments at this pH.

We proceeded by determining an accurate TON and TOF for our other nickel catalysts (Figure 3). Catalyst **1** contains two imine donor groups instead of two (of the four) amine groups in catalysts **2** and **3**. Apparently these imine functionalities make catalyst **1** significantly faster than **2**, which in turn is more active than the methylated meso complex **3**. Interestingly, catalyst **6**, which has a non-methylated BPMEN ligand, is slower than the cyclam-based systems but remains stable for a longer time, still producing oxygen after 30 min. To confirm the existence of a ligand effect on the water oxidation catalysis activity of the nickel complexes, we evaluated several nickel salts [NiCl$_2$, Ni(OAc)$_2$, Ni(ClO$_4$)$_2$, Ni(NO$_3$)$_2$] and nickel oxide nanoparticles ($\approx$ 20 nm in diameter) under the same conditions (Figure 3 and Supporting Information, Figure S2). None of these systems shows any oxygen evolution. This lack of activity indicates that the nickel complexes operate as molecular species in which the ligand influences the activity and stability. To confirm that the formed oxygen originates from water and not from decomposition of Oxone, we performed oxygen evolution experiments with O^{18}-labeled water. This experiment reveals a significant increase in O$_2^{36}$ compared to O$_2^{34}$, indicating that the proposed complex is capable of oxidizing water (Supporting Information, Figure S3). Unfortunately, due
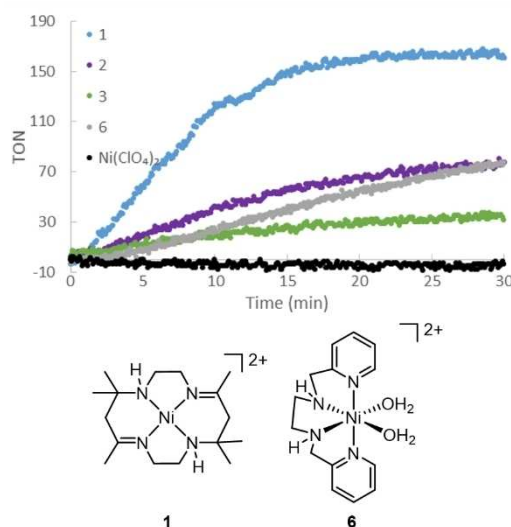
to leakage, no reliable quantification of a ratio between O$_2^{32}$ and the other isotopes could be achieved.

After establishing the importance and influence of the ligand that is coordinated to nickel, we systematically varied the ligand framework to establish structure-activity relationships. In Figure 4 we report an overview of the cyclam-based complexes we have investigated for this study (several additional inactive complexes are reported in the Supporting Information, Figure S4). Complex **1** with two imine donor ligands is the most active with a TON of 170 and a TOF of 13 min^{-1}. Imine donor ligands are rarely utilized in water oxidation catalysts, with the exception of cobalt and manganese Schiff base complexes and several binuclear iridium and ruthenium systems.[80–84] Cyclam ligands with methylated bridging propane moieties produce a less active catalyst (both in terms of TOF and TON), as becomes
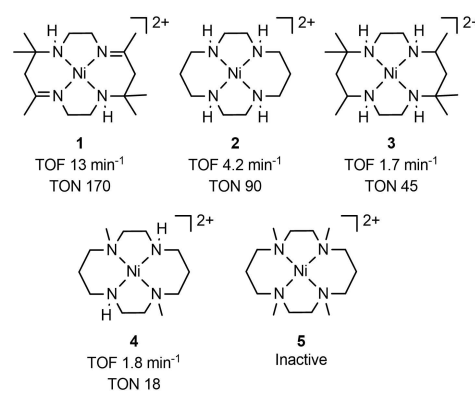
Figure 4. Nickel complexes **1**–**5** and their oxygen evolution activity at a concentration of 0.10 mM nickel using 0.10 M Oxone as oxidant in a pH 5.0 acetate buffer (TOF and TON determined by manometry).

clear by comparing complexes **2** and **3**. The methylation of nitrogen donor atoms also has a negative effect on the activity, as complex **4** is less active than **2**, and **5** does not show any activity. For iron- and manganese-based catalysts, tertiary amines are usually better donor groups for oxidation catalysts than secondary amines. This is not observed for our series of nickel complexes.[67,85] However, the trend in activity does correspond with the trend in oxidation potentials of the nickel complexes. The Ni^{III}/Ni^{II} oxidation wave in acetic acid buffer at pH 5.0 is at 0.77 V vs. normal hydrogen electrode (NHE) for complex **2**, at 0.98 V vs. NHE for complex **3**, and at 1.06 and 1.57 V vs. NHE for complexes **4** and **5**, respectively (Supporting Information, Figure S5). At lower Ni^{III}/Ni^{II} oxidation potential, a higher activity is observed. The oxidation potential of the nickel complexes follows the same trend in organic solvents.[86] In addition, tertiary amines coordinate weaker to nickel(III) species by about two orders of magnitude.[87] This weaker coordination could result in faster decomposition, which may explain the lower TONs observed for the complexes with tertiary amine donors.

When comparing BPMEN-type complexes **6–9**, similar trends are found as for the cyclam series (Figure 5). In the BPMEN series, complex **6**, which has a ligand based on secondary amine donor groups, reveals the highest activity with a TOF of 3 min^{-1} and a TON of 136. In line with the observed trend for cyclam complexes, catalyst **8** with tertiary amine ligands demonstrates a lower activity than complex **6**, which contains two secondary amine donor ligands. Contrary to the trend in cyclam-based systems, imine-based complex **7** is less active than **6** (Figure 5, TOFs **1** and **3** respectively). Complex **8** with non-coordinating perchlorate counterions and a TOF of 0.25 min^{-1} is more than twice as fast as complex **9** with coordinating chloride anions, which displays a TOF of only 0.11 min^{-1}. This observation is in line with trends found for other first-row transition metals.[49] A complex with three pyridine donors does not show any activity in oxygen evolution (Figure 5, **10**). For iron-based complexes the trends are different
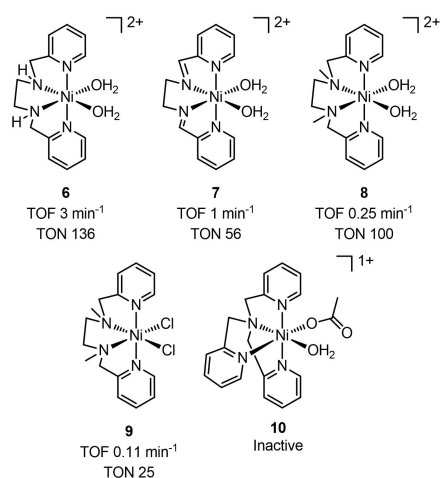
to those observed for nickel complexes. An iron BPMEN-imine complex is inactive, a BPMEN complex with secondary amine donors shows minor activity, while an iron complex with tertiary amine donors reveals high activity.[49,67] This discrepancy in design rules has important consequences for catalyst design because often ligand frameworks and design rules that work well for one metal are also applied to other metals.[52] Here we show that such extrapolations are inappropriate, and trends and ligand design rules should be re-established for different metals.

To gain some initial understanding of the mechanism involved in nickel-catalyzed water oxidation we subjected complexes **1** and **2** to kinetic analysis. Using 0.10 mM complex **1** with oxidant concentrations varying from 0.05 until 0.50 M, we observed a first-order rate dependency on the oxidant concentration (Figure 6a), with the highest TOF of 68 min^{-1} at 0.50 M of Oxone. Nickel cyclam complex **2** also shows a first order in Oxone (Supporting Information, Figure S6). The first-order rate dependency on oxidant concentration implies that Oxone is involved in the rate-limiting step. Therefore, it is likely that one of the oxidation steps is rate-determining and not O—O bond formation, which is often assumed to be rate-limiting.[35,45] As the O—O bond formation is not the rate-determining step, it is difficult to establish from the kinetics if this nickel catalyst follows the mononuclear water nucleophilic attack or the dinuclear radical oxo coupling mechanism.[19,23]

The order in **1** was determined by performing water oxidation at different complex concentrations. Figure 6b shows that the data can be linearly fitted if we plot the oxygen

6
TOF 3 min^{-1}
TON 136

7
TOF 1 min^{-1}
TON 56

8
TOF 0.25 min^{-1}
TON 100

9
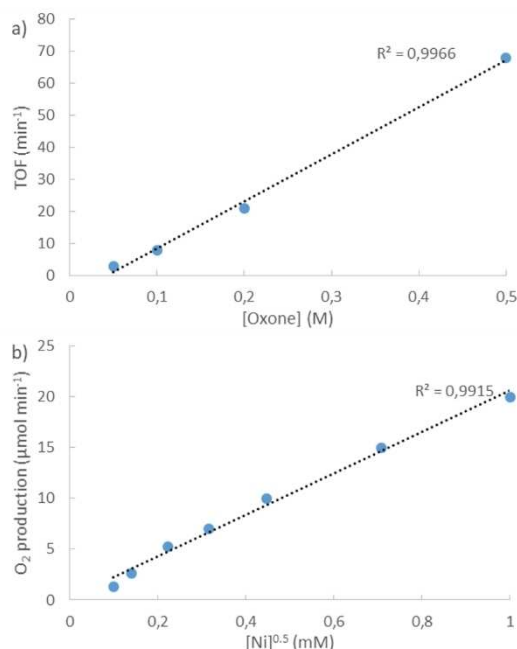TOF 0.11 min^{-1}
TON 25

10
Inactive

Figure 5. Nickel complexes **6–10** and their oxygen evolution activity at a concentration of 0.10 mM nickel using 0.10 M Oxone as oxidant in a pH 5.0 acetate buffer (TOF and TON determined by manometry).

Figure 6. Kinetic studies with nickel complex **1**. a) TOFs per minute of 0.10 mM **1** using various Oxone concentrations in a 1.0 M acetate buffer at a pH of 5.0. b) Rate of oxygen evolution versus the square root of the concentration of **1** in a 0.50 M acetate buffer at a pH of 5.0 using 0.10 M of Oxone as oxidant.

ChemSusChem

Full Papers
doi.org/10.1002/cssc.202002164

**Chemistry
Europe**
European Chemical
Societies Publishing

evolution rate versus the square root of the catalyst concentration. This reveals a half-order dependency on catalyst concentration at an oxidant concentration of 0.10 M on the O_2 production rate. Complex **2** has the same half-order dependence on the catalyst concentration (Supporting Information, Figure S6). The broken order typically indicates the existence of a pre-equilibrium between a dimer and monomer species, before the rate-determining step. Dimeric oxygen-bridged nickel complexes are known in literature, and both μ-O bridged[88,89] and μ-O_2 bridged species have been reported.[90,91] Interestingly, Kieber-Emmons and Riordan reported nickel complexes that activate molecular oxygen and, depending on steric bulk around the nickel center, result in either a dimeric Ni–(μ–O)$_2$–Ni species or a monomeric Ni–μ–O_2 species.[92] In the same paper they show that the equilibrium is shifted towards the monomeric species by introducing more steric bulk in the ligands. A half order in catalyst concentration for water oxidation has also been observed for an iridium-based system by Hintermair and co-workers.[93] The authors attribute this kinetic profile to an out-of-cycle dimeric Ir species. If such an out-of-cycle dimer also exists in our nickel-based reaction, the rate of catalysis could be improved by shifting the equilibrium to the monomeric state. Following the work of Kieber-Emmons and Riordan,[92] an increase of steric bulk could result in this shift and should lead to more monomeric species and thus faster oxygen evolution catalysis. Next to information about reaction kinetics, the last series of experiments performed at different catalyst concentrations also provided information about catalyst stability. We observe higher TONs, up to 380, at lower catalyst concentrations (Supporting Information, Figures S7 and S8). However, the oxidant consumption never exceeds 50 %, indicating that catalyst stability needs further improvement.

Conclusions

In this work we show that water oxidation activity of nickel-based complexes can be evaluated by driving the reaction with Oxone as a chemical oxidant. Importantly, nickel salts and nickel oxide nanoparticles are inactive under these conditions, and thus any activity stems from the molecular complexes. We show that known water oxidation catalysts like **2** and **3**, based on cyclam-type ligands, are surpassed in activity by complex **1** that is based on a ligand with imine donor groups. In addition, secondary amine donor groups result in a more active catalyst than tertiary amine donor groups (**2** > **4** > **5** and **6** > **8**) for all examined complexes. This trend is opposite to that observed for iron-based complexes. Based on this observation we can conclude that design rules for water oxidation catalysts are not universal among different transition metals. Kinetic studies with the most active nickel complex (**1**) reveal a first order in oxidant and a half order in catalyst. This implies that the oxidation of the catalytic species is the rate-determining step, which is preceded by the breaking up of a dimeric nickel species. With this work we establish some structure-activity relationships for

nickel-based water oxidation catalysts, which may guide future directions in this promising research area.

Experimental Section

Experimental details and additional kinetic data are available in the Supporting Information.

Conflict of Interest

The authors declare no conflict of interest.

[1] N. S. Lewis, D. G. Nocera, *Proc. Mont. Acad. Sci.* **2006**, *103*, 15729–15735.
[2] B. Zhang, L. Sun, *Chem. Soc. Rev.* **2019**, *48*, 2216–2264.
[3] R. J. Detz, J. N. H. Reek, B. C. C. Van Der Zwaan, *Energy Environ. Sci.* **2018**, *11*, 1653–1669.
[4] J. Gong, C. Li, M. R. Wasielewski, *Chem. Soc. Rev.* **2019**, *48*, 1862–1864.
[5] R. J. Detz, K. Sakai, L. Spiccia, G. W. Brudvig, L. Sun, J. N. H. Reek, *ChemPlusChem* **2016**, *81*, 1024–1027.
[6] S. Berardi, S. Drouet, L. Francàs, C. Gimbert-Suriñach, M. Guttentag, C. Richmond, T. Stoll, A. Llobet, *Chem. Soc. Rev.* **2014**, *43*, 7501–7519.
[7] D. L. Dubois, *Inorg. Chem.* **2014**, *53*, 3935–3960.
[8] A. J. Esswein, D. G. Nocera, *Chem. Rev.* **2007**, *107*, 4022–4047.
[9] J. Qiao, Y. Liu, F. Hong, J. Zhang, *Chem. Soc. Rev.* **2014**, *43*, 631–675.
[10] A. J. Morris, G. J. Meyer, E. Fujita, *Acc. Chem. Res.* **2009**, *42*, 1983–1994.
[11] N. Elgrishi, M. B. Chambers, X. Wang, M. Fontecave, *Chem. Soc. Rev.* **2017**, *46*, 761–796.
[12] E. E. Benson, C. P. Kubiak, A. J. Sathrum, J. M. Smieja, *Chem. Soc. Rev.* **2009**, *38*, 89–99.
[13] L. Chen, Z. Guo, X.-G. Wei, C. Gallenkamp, J. Bonin, E. Anxolabéhère-Mallart, K.-C. Lau, T.-C. Lau, M. Robert, *J. Am. Chem. Soc.* **2015**, *137*, 10918–10921.
[14] A. Singh, L. Spiccia, *Coord. Chem. Rev.* **2013**, *257*, 2607–2622.
[15] R. Matheu, P. Garrido-Barros, M. Gil-Sepulcre, M. Z. Ertem, X. Sala, C. Gimbert-Suriñach, A. Llobet, *Nat. Rev. Chem.* **2019**, *3*, 331–341.
[16] X. Sala, S. Maji, R. Bofill, J. García-Antón, A. Escriche, A. Llobet, *Acc. Chem. Res.* **2014**, *47*, 504–516.
[17] N.-T. Suen, S.-F. Hung, Q. Quan, N. Zhang, Y.-J. Xu, H. M. Chen, *Chem. Soc. Rev.* **2017**, *46*, 337–365.
[18] J. Li, R. Güttinger, R. Moré, F. Song, W. Wan, G. R. Patzke, *Chem. Soc. Rev.* **2017**, *46*, 6124–6147.
[19] M. D. Kärkäs, O. Verho, E. V. Johnston, B. Åkermark, *Chem. Rev.* **2014**, *114*, 11863–12001.
[20] J. D. Blakemore, R. H. Crabtree, G. W. Brudvig, *Chem. Rev.* **2015**, *115*, 12974–13005.
[21] D. J. Wasylenko, R. D. Palmer, C. P. Berlinguette, *Chem. Commun.* **2013**, *49*, 218–227.
[22] D. G. H. Hetterscheid, J. N. H. Reek, *Angew. Chem. Int. Ed.* **2012**, *51*, 9740–9747; *Angew. Chem.* **2012**, *124*, 9878–9885.
[23] Y. Li, X. Bao, D. Chen, Z. Wang, N. Dewangan, M. Li, Z. Xu, J. Wang, S. Kawi, Q. Zhong, *ChemCatChem* **2019**, *11*, 5913–5928.

[24] T. Smolinka, E. T. Ojong, J. Garche in *Electrochemical Energy Storage for Renewable Sources and Grid Balancing*, Elsevier B. V., **2015**, pp. 103–128.

[25] Y. Umena, K. Kawakami, J.-R. Shen, N. Kamiya, *Nature* **2011**, *473*, 55–60.

[26] P. E. M. Siegbahn, *Proc. Mont. Acad. Sci.* **2017**, *114*, 4966–4968.

[27] M. Suga, F. Akita, K. Yamashita, Y. Nakajima, G. Ueno, H. Li, T. Yamane, K. Hirata, Y. Umena, S. Yonekura, L.-J. Yu, H. Murakami, T. Nomura, T. Kimura, M. Kubo, S. Baba, T. Kumasaka, K. Tono, M. Yabashi, H. Isobe, K. Yamaguchi, M. Yamamoto, H. Ago, J.-R. Shen, *Science* **2019**, *366*, 334–338.

[28] M. Shamsipur, A. Pashabadi, *Coord. Chem. Rev.* **2018**, *374*, 153–172.

[29] P. W. N. M. van Leeuwen, in *Homogeneous Catalysis*, Kluwer Acedemic Publishers, **2004**.

[30] M. L. Helm, M. P. Stewart, R. M. Bullock, M. R. DuBois, D. L. DuBois, *Science* **2011**, *333*, 863–866.

[31] Y. Wang, Z. Wang, Y. Li, G. Wu, Z. Cao, L. Zhang, *Nat. Commun.* **2014**, *5*, 3470.

[32] A. M. Allgeier, C. A. Mirkin, *Angew. Chem. Int. Ed.* **1998**, *37*, 894–908; *Angew. Chem.* **1998**, *110*, 936–952.

[33] P. Garrido-Barros, C. Gimbert-Suriñach, R. Matheu, X. Sala, A. Llobet, *Chem. Soc. Rev.* **2017**, *46*, 6088–6098.

[34] J. Hessels, R. J. Detz, M. T. M. Koper, J. N. H. Reek, *Chem. Eur. J.* **2017**, *23*, 16413–16418.

[35] T. Kikuchi, K. Tanaka, *Eur. J. Inorg. Chem.* **2014**, *4*, 607–618.

[36] F. Yu, D. Poole, S. Mathew, N. Yan, J. Hessels, N. Orth, I. Ivanović-Burmazović, J. N. H. Reek, *Angew. Chem. Int. Ed.* **2018**, *57*, 11247–11251; *Angew. Chem.* **2018**, *130*, 11417–11421.

[37] Y. Xie, D. W. Shaffer, J. J. Concepcion, *Inorg. Chem.* **2018**, *57*, 10533–10542.

[38] J. Kamdar, D. Grotjahn, *Molecules* **2019**, *24*, 494.

[39] R. Matheu, M. Z. Ertem, J. Benet-Buchholz, E. Coronado, V. S. Batista, X. Sala, A. Llobet, *J. Am. Chem. Soc.* **2015**, *137*, 10786–10795.

[40] L. Duan, F. Bozoglian, S. Mandal, B. Stewart, T. Privalov, A. Llobet, L. Sun, *Nat. Chem.* **2012**, *4*, 418–423.

[41] J. D. Blakemore, N. D. Schley, D. Balcells, J. F. Hull, G. W. Olack, C. D. Incarvito, O. Eisenstein, G. W. Brudvig, R. H. Crabtree, *J. Am. Chem. Soc.* **2010**, *132*, 16017–16029.

[42] J. A. Woods, R. Lalrempuia, A. Petronilho, N. D. McDaniel, H. Müller-Bunz, M. Albrecht, S. Bernhard, *Energy Environ. Sci.* **2014**, *7*, 2316–2328.

[43] S. W. Sheehan, J. M. Thomsen, U. Hintermair, R. H. Crabtree, G. W. Brudvig, C. A. Schmuttenmaer, *Nat. Commun.* **2015**, *6*, 6469.

[44] M. D. Kärkäs, B. Åkermark, *Dalton Trans.* **2016**, *45*, 14421–14461.

[45] N. Wang, H. Zheng, W. Zhang, R. Cao, *Chin. J. Catal.* **2018**, *39*, 228–244.

[46] S. M. Barnett, C. R. Waidmann, M. L. Scheuermann, J. C. Nesvet, K. Goldberg, J. M. Mayer in *Molecular Water Oxidation Catalysis: A Key Topic for New Sustainable Energy Conversion Schmes* (Ed.: A. Llobet), Wiley, **2014**, pp. 187–210.

[47] M. Kondo, S. Masaoka, *Chem. Lett.* **2016**, *45*, 1220–1231.

[48] T. Liu, B. Zhang, L. Sun, *Chem. Asian J.* **2019**, *14*, 31–43.

[49] J. Lorret-Fillol, Z. Codolà, I. Garcia-Bosch, L. Gómez, J. J. Pla, M. Costas, *Nat. Chem.* **2011**, *3*, 807–813.

[50] K. Zeng, D. Zhang, *Prog. Energy Combust. Sci.* **2010**, *36*, 307–326.

[51] M. Zhang, M.-T. Zhang, C. Hou, Z.-F. Ke, T.-B. Lu, *Angew. Chem. Int. Ed.* **2014**, *53*, 13042–13048; *Angew. Chem. Int. Ed.* **2014**, *126*, 13258–13264.

[52] G.-Y. Luo, H.-H. Huang, J.-W. Wang, T.-B. Lu, *ChemSusChem* **2016**, *9*, 485–491.

[53] J.-W. Wang, X.-Q. Zhang, H.-H. Huang, T.-B. Lu, *ChemCatChem* **2016**, *8*, 3287–3293.

[54] J.-W. Wang, C. Hou, H.-H. Huang, W.-J. Liu, Z.-F. Ke, T.-B. Lu, *Catal. Sci. Technol.* **2017**, *7*, 5585–5593.

[55] B. Ariela, W. Yaniv, S. Dror, K. Haya, A. Yael, M. Eric, M. Dan, *Dalton Trans.* **2017**, *46*, 10774–10779.

[56] Y. Han, Y. Wu, W. Lai, R. Cao, *Inorg. Chem.* **2015**, *54*, 5604–5613.

[57] L. Wang, L. Duan, R. B. Ambre, Q. Daniel, H. Chen, J. Sun, B. Das, A. Thapper, J. Uhlig, P. Dinér, L. Sun, *J. Catal.* **2016**, *335*, 72–78.

[58] L.-H. Zhang, F. Yu, Y. Shi, F. Li, H. Li, *Chem. Commun.* **2019**, *55*, 6122–6125.

[59] G. Azadi, Z. Zand, Y. Mousazade, R. Bagheri, J. Cui, Z. Song, R. Bikas, K. Wozniak, S. I. Allakhverdiev, M. M. Najafpour, *Int. J. Hydrogen Energy* **2019**, *44*, 2857–2867.

[60] J. Lin, P. Kang, X. Liang, B. Ma, Y. Ding, *Electrochim. Acta* **2017**, *258*, 353–359.

[61] P. Garrido-Barros, S. Grau, S. Drouet, J. Benet-Buchholz, C. Gimbert-Suriñach, A. Llobet, *ACS Catal.* **2019**, *9*, 3936–3945.

[62] D. Wang, C. O. Bruner, *Inorg. Chem.* **2017**, *56*, 13638–13641.

[63] J. Shen, M. Wang, T. He, J. Jiang, M. Hu, *Chem. Commun.* **2018**, *54*, 9019–9022.

[64] Y. Liu, R. Xiang, X. Du, Y. Ding, B. Ma, *Chem. Commun.* **2014**, *50*, 12779–12782.

[65] G. Chen, L. Chen, S.-M. Ng, T.-C. Lau, *ChemSusChem* **2014**, *7*, 127–134.

[66] D. Hong, S. Mandal, Y. Yamada, Y.-M. Lee, W. Nam, A. Llobet, S. Fukuzumi, *Inorg. Chem.* **2013**, *52*, 9522–9531.

[67] R. J. Detz, Z. Abiri, A. M. Kluwer, J. N. H. Reek, *ChemSusChem* **2015**, *8*, 3057–3061.

[68] D. G. H. Hetterscheid, J. N. H. Reek, *Chem. Commun.* **2011**, *47*, 2712–2714.

[69] A. R. Parent, T. Nakazono, S. Lin, S. Utsunomiya, K. Sakai, *Dalton Trans.* **2014**, *43*, 12501–12513.

[70] J. M. Koelewijn, M. Lutz, W. I. Dzik, R. J. Detz, J. N. H. Reek, *ACS Catal.* **2016**, *6*, 3418–3427.

[71] J. Limburg, J. S. Vrettos, H. Chen, J. C. De Paula, R. H. Crabtree, G. W. Brudvig, *J. Am. Chem. Soc.* **2001**, *123*, 423–430.

[72] R. Tagore, R. H. Crabtree, G. W. Brudvig, *Inorg. Chem.* **2008**, *47*, 1815–1823.

[73] R. K. Seidler-Egdal, A. Nielsen, A. D. Bond, M. J. Bjerrum, C. J. McKenzie, *Dalton Trans.* **2011**, *40*, 3849–3858.

[74] M. M. Najafpour, W. Hillier, A. N. Shamkhali, M. Amini, K. Beckmann, Z. Jagličić, M. Jagodič, P. Strauch, A. N. Moghaddam, G. Beretta, M. Bagherzadeh, *Dalton Trans.* **2012**, *41*, 12282–12288.

[75] K. J. Young, M. K. Takase, G. W. Brudvig, *Inorg. Chem.* **2013**, *52*, 7615–7622.

[76] W.-P. To, T. W.-S. Chow, C.-W. Tse, X. Guan, J.-S. Huang, C.-M. Che, *Chem. Sci.* **2015**, *6*, 5891–5903.

[77] L. Mognon, S. Mandal, C. E. Castillo, J. Fortage, F. Molton, G. Aromí, J. Benet-Buchhlolz, M.-N. Collomb, A. Llobet, *Chem. Sci.* **2016**, *7*, 3304–3312.

[78] C. Panda, J. Debgupta, D. D. Díaz, K. K. Singh, S. S. Gupta, B. B. Dhar, *J. Am. Chem. Soc.* **2014**, *136*, 12273–12282.

[79] A. Chirila, M. B. Brands, J. de Bruin, *J. Catal.* **2018**, *361*, 347–360.

[80] M. A. Asraf, H. A. Younus, C. I. Ezugwu, A. Mehta, F. Verpoort, *Catal. Sci. Technol.* **2016**, *6*, 4271–4282.

[81] F. M. Ashmawy, C. A. McAuliffe, R. V. Parish, J. Tames, *J. Chem. Soc. Dalton Trans.* **1985**, *7*, 1391–1397.

[82] G. González-Riopedre, M. I. Fernández-García, A. M. González-Noya, M. Á. Vázquez-Fernández, M. R. Bermejo, M. Maneiro, *Phys. Chem. Chem. Phys.* **2011**, *13*, 18069–18077.

[83] W. I. Dzik, S. E. Calvo, J. N. H. Reek, M. Lutz, M. A. Ciriano, C. Tejel, D. G. H. Hetterscheid, B. De Bruin, *Organometallics* **2011**, *30*, 372–374.

[84] P. Li, J.-B. Liu, S. Han, W. Deng, Z.-J. Yao, *Appl. Organomet. Chem.* **2019**, *33*, e5040.

[85] N. C. Maity, P. K. Bera, D. Ghosh, S. H. R. Abdi, R. I. Kureshy, N. H. Khan, H. C. Bajaj, E. Suresh, *Catal. Sci. Technol.* **2014**, *4*, 208–217.

[86] E. K. Barefield, G. M. Freeman, D. G. Van Derveer, *Inorg. Chem.* **1986**, *25*, 552–558.

[87] D. Shamir, I. Zilbermann, E. Maimon, D. Meyerstein, *Eur. J. Inorg. Chem.* **2004**, 4002–4005.

[88] S. Hikichi, M. Yoshizawa, Y. Sasakura, M. Akita, Y. Moro-Oka, *J. Am. Chem. Soc.* **1998**, *120*, 10567–10568.

[89] S. K. Padamati, D. Angelone, A. Draksharapu, G. Primi, D. J. Martin, M. Tromp, M. Swart, W. R. Browne, *J. Am. Chem. Soc.* **2017**, *139*, 8718–8724.

[90] M. T. Kieber-Emmons, R. Schenker, G. P. A. Yap, T. C. Brunold, C. G. Riordan, *Angew. Chem. Int. Ed.* **2004**, *43*, 6716–6718; *Angew. Chem.* **2004**, *116*, 6884–6886.

[91] M. T. Kieber-Emmons, J. Annaraj, M. S. Seo, K. M. Van Heuvelen, T. Tosha, T. Kitagawa, T. C. Brunold, W. Nam, C. G. Riordan, *J. Am. Chem. Soc.* **2006**, *128*, 14230–14231.

[92] M. T. Kieber-Emmons, C. G. Riordan *Acc. Chem. Res.* **2007**, *40*, 618–625.

[93] E. V. Sackville, F. Marken, U. Hintermair, *ChemCatChem* **2018**, *10*, 4280–4291.